

Adsorption characteristics of uranyl ions by manganese oxide coated sand in batch mode

Weihua Zou · Lei Zhao · Runping Han

Received: 24 October 2010 / Published online: 23 December 2010
© Akadémiai Kiadó, Budapest, Hungary 2010

Abstract In this paper, the sorption properties of manganese oxide coated sand (MOCS) towards uranium(VI) from aqueous solutions were studied in a batch adsorption system. Scanning electron microscope (SEM) and infrared (IR) analyses were used to characterize MOCS. Parameters affecting the adsorption of uranium(VI), such as the contact time, salt concentration, competitive ions, temperature and initial uranium(VI) concentration, were investigated. The equilibrium adsorption data were analyzed by Langmuir, Freundlich and Redlich–Peterson models using nonlinear regressive analysis. The results indicated that the Langmuir and Redlich–Peterson models provided the best correlation of experimental data. The kinetic experimental data were analyzed using three kinetic equations including pseudo-first order equation, pseudo-second order equation and intraparticle diffusion model to examine the mechanism of adsorption and potential rate-controlling step. The process mechanism was found to be complex, consisting of both surface adsorption and pore diffusion. The effective diffusion parameter D_i values estimated in the order of $10^{-7} \text{ cm}^2 \text{ s}^{-1}$ indicated that the intraparticle diffusion was not the rate-controlling step. Thermodynamic study showed that the adsorption was a spontaneous, endothermic process. Adsorbed U(VI) ions were desorbed effectively (about 94.7%) by 0.1 mol L⁻¹ HNO₃. The results

indicated that MOCS can be used as an effective adsorbent for the treatment of industrial wastewaters contaminated with U(VI) ions.

Keywords Manganese oxide coated sand · Uranium(VI) · Adsorption isotherm · Kinetic model · Desorption

Introduction

The removal of contaminating uranium(VI) ions from the environment is one of serious concern because of their associated radioactivity and toxicity. Uranium and its compounds are all highly toxic, which is a threat to human health and ecological balance. Hence, research into the separation of U(VI) ions from wastewater is important. Many processes have been proposed for U(VI) ion removal from industrial wastewaters and radioactive wastes, with chemical precipitation, ion-exchange, membrane processes, solvent extraction and adsorption being the most commonly used methods employed [1–5].

Manganese oxides, with high adsorptive property, are usually considered as the most important scavengers for trace metals in soil, sediments, and rocks. In the presence of water, the surfaces of manganese oxides are covered with surface hydroxyl groups, protons and coordinated water molecules. Such surfaces have large surface areas, a microporous structure, high pH-dependent surface charges and a large number of binding sites. As a consequence, they have a significant impact on contaminant mobility [6, 7], providing an efficient scavenging pathway for heavy metal ions in toxic systems. However, the use of pure manganese oxide as a filter media is not practical both from economic reasons and because of its unfavourable physical and chemical characteristics. Furthermore, the fine particle

W. Zou (✉) · L. Zhao
School of Chemical Engineering, Zhengzhou University,
100# of Kexue Road, Zhengzhou, Henan 450001,
People's Republic of China
e-mail: whzou@zzu.edu.cn

R. Han (✉)
Department of Chemistry, Zhengzhou University, 100# of Kexue
Road, Zhengzhou, Henan 450001, People's Republic of China
e-mail: rphan67@zzu.edu.cn

size of manganese oxides makes it very difficult to separate the solid from the aqueous phase or to allow ready penetration through the bed. However, coating manganese oxide onto a support surface may provide an effective and promising means for the removal of heavy metal ions from wastewater.

Silica sand is a common conventional filter media because of its cheapness, inertness, and availability. However, because of the poor efficiency of silica sand towards the adsorption heavy metal ions from solution, modifications are needed to improve its adsorption capacity. In order to overcome the lack of strength of pure manganese oxide and to enhance the treatment efficiency and its capability of removing radioactive metal ions, a modified method of coating manganese oxides onto sand surfaces has been developed. This method of coating sand with a thin layer of manganese oxide enhances its sorption capacity towards metal ions relative to uncoated sand. The enhanced capacity towards pollutant removal is a result of increased surface area and the amphoteric surface charge provided by coating the sand [8–11].

The research described herein was designed to investigate the characteristics of MOCS and to test the properties of MOCS as an adsorbent for removing U(VI) ions from synthetic solutions via a batch system. The data relating to the adsorption capacities of MOCS were examined using the Langmuir isotherm equation. Further, the kinetics and the mechanistic steps involved in the sorption process were evaluated at different initial uranium(VI) concentrations. The adsorption capacity of the adsorbents used in the present work was also compared with other adsorbents used by different researchers. In addition, the regeneration and reusability of the adsorbent was also evaluated.

Experimental

Materials

Adsorbents

Quartz sand, as provided by Zhengzhou's Company, Zhengzhou, P.R. China, possesses grains with diameter in the range 0.99–0.67 mm. The sand particles were soaked in a 0.1 mol L⁻¹ hydrochloric acid solution for 24 h, rinsed with distilled water and then dried in an oven at 373 K prior to surface coating. Manganese oxide coated sand (MOCS) was obtained by utilizing a reductive procedure modified to precipitate manganese oxide colloids on the surfaces of the quartz sand particle. Thus, a boiling solution containing potassium permanganate was poured over dried sand particles placed in a beaker and then hydrochloric acid (37.5%, W_{HCl}/W_{H₂O}) was added dropwise into the solution. After

stirring for 1 h, the mixture was filtered, washed with distilled water to attain a pH value of 7.0, dried at room temperature, and stored in polypropylene bottle prior to use.

Reagents

All chemicals and reagents used for experiments and analyses were of A.R. grade. A stock 1,000 mg L⁻¹ solution of U(VI) ions was prepared by dissolving an appropriate amount of A.R. UO₂(NO₃)₂·6H₂O in deionized water. The initial pH values of the working solutions were adjusted by addition of HNO₃ or NaOH solution. Arsenazo III solution was prepared by dissolving 0.5 g of the reagent in 1,000 mL of deionized water. Fresh dilutions were employed for each sorption study.

Determination of uranium contents in solution

A simple and sensitive spectrophotometric method based on colored complexes with Arsenazo III in an aqueous medium was used for the determination U(VI) ion concentration [12]. The concentration of U(VI) ions in solution was determined spectrophotometrically by absorbance measurements at λ_{max} of 588 nm using a Shimadzu Brand UV-3000 spectrophotometer.

Adsorption and desorption experiments

Batch sorption experiments were undertaken by shaking flasks containing the appropriate solutions and adsorbent at 120 rpm for a known period of time employing a mechanical shaker in conjunction with a water bath.

The amount of adsorbed U(VI) ions per gram MOCS was obtained using the following expression:

$$q = v(C_0 - C_f)/m \quad (1)$$

where q is the amount of U(VI) ions adsorbed on MOCS (mg g⁻¹), C_0 and C_f are the concentrations of U(VI) ions in the solution (mg L⁻¹) prior to and adsorption. v is the volume of the aqueous phase (L), and m is the dry weight of MOCS (g).

Effect of pH on adsorption

The effect of pH on the adsorption capacity of MOCS was investigated using solutions U(VI) ion solution of initial concentration 10, 20 and 40 mg L⁻¹, respectively, at 288 K and varying the initial pH values within the range 2–11. For such experiments, a 5.0 g L⁻¹ solution of MOCS was added to 10 mL of the corresponding U(VI) ion solutions. Flasks were agitated on a shaker for 180 min at a constant agitation speed of 120 rpm to ensure equilibrium was reached.

Effect of salt concentrations on U(VI) adsorption

The concentration of NaNO_3 , KNO_3 , $\text{Ca}(\text{NO}_3)_2$ were used ranged from 0 to 0.1 mol L⁻¹. The initial concentration of U(VI) was 20 mg L⁻¹, and contact time was 180 min at the temperature of 288 K. An initial pH of U(VI) solution was 5.0.

Effect of copper and zinc competition on U(VI) adsorption

Studies of competitive adsorption were performed at an initial pH of 6.0 at 288 K. In two series of solutions, the initial concentration of Cu(II) or Zn(II) were fixed to 10, 20, and 40 mg L⁻¹, whereas the concentrations of U(VI) were varied from 10 to 60 mg L⁻¹. After equilibrium, the concentration of residual U(VI) ions in solution was analyzed.

Equilibrium studies

Equilibrium adsorption experiments were carried out at a pH of 5.0 employing U(VI) ion solutions with initial concentrations within the range 10–100 mg L⁻¹ for U(VI) ions at 288, 303 and 318 K. After 180 min, the aqueous phase was separated from MOCS, and the corresponding supernatants collected. The concentration of U(VI) ions in the supernatants were measured.

Kinetic studies

For kinetic experiments, the flasks containing 10 mL of U(VI) ions solution of 10, 20, 40 mg L⁻¹ and 5 g L⁻¹ MOCS were subjected to agitation using water bath shakers for different contact time intervals. The flasks were taken from the shakers at regular time intervals and the remaining concentration of U(VI) ions in the supernatants was estimated.

Desorption studies

In order to determine the reusability of the adsorbent, consecutive adsorption–desorption cycles were repeated four times. 0.1 mol L⁻¹ HNO_3 was used as the desorbing agent. MOCS loaded with U(VI) ions was placed in the desorbing medium and was constantly stirred at 120 rpm for 150 min at 288 K. After each cycle of adsorption and desorption, MOCS was washed with deionized water and reconditioned for adsorption in the succeeding cycle.

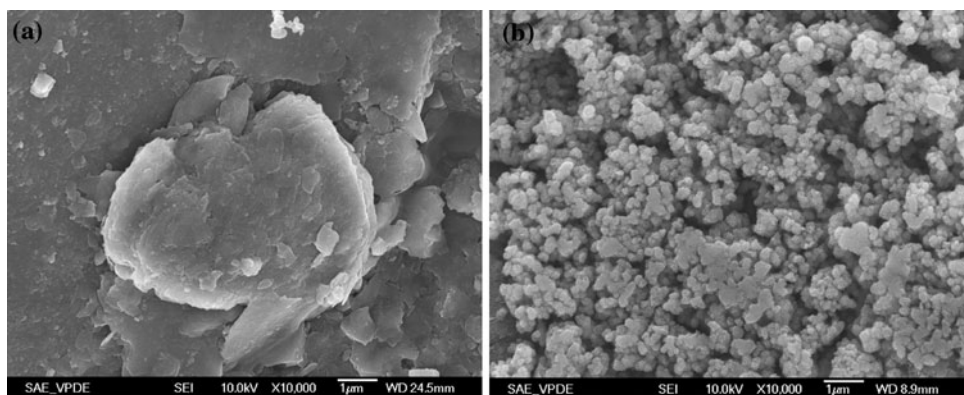
Results and discussion

Characteristics of manganese oxide

SEM image showed that the quartz sand had a relatively uniform and smooth surface (Fig. 1). The coated sand surfaces were apparently occupied by nascent manganese oxides formed during the coating process. The amount of manganese on the surface of MOCS was ca. 5.46 mg Mn/g sand. After coating the surfaces of the sand particles with manganese oxides, the specific surface area increased from 0.674 to 0.712 m² g⁻¹. This may have been caused by an increase in both the inner and surface porosity after adding the manganese oxides admixture [10].

The IR spectra for manganese oxides (scrape from the surface of MOCS) of unadsorbed and adsorbed of U(VI) ions is shown in Fig. 2a and b. As shown in Fig. 2a, three bands were observed in the region of 400–4000 cm⁻¹. The presence of a broad and strong band near 3423 cm⁻¹, together with a relatively sharp band at about 1630 cm⁻¹ in the spectrum is assigned to the stretching and bending stretching vibration of –OH in H₂O. The broad band at the region from 3600 to 3000 cm⁻¹ in the IR spectrum indicated that the hydroxyl group may be existed in the manganese oxide structure [13]. Hydroxyl groups are active surface sites for adsorption or ion exchange. The peak located at 528 cm⁻¹ is characteristics of the stretching

Fig. 1 SEM micrograph of sample: **a** sand and **b** MOCS



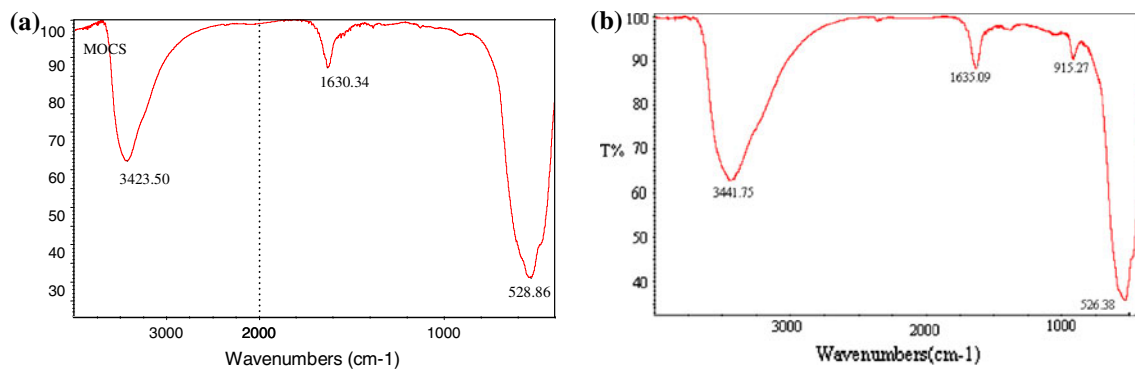


Fig. 2 IR spectra of MOCS **a** as prepared without adsorbed U(VI) ions and **b** with adsorbed U(VI) ions

vibration of Mn–O, which can matched with the spectra of birnessite [14].

By comparing the IR spectra of manganese oxide before and after adsorption of U(VI), it was seen that a sharp peak at 915 cm^{-1} corresponding to $\nu_{\text{U}-\text{O}}$ of uranyl ion appeared, which is a direct evidence for that manganese oxide adsorbed U(VI) under the present experimental conditions [15, 16].

The effect of pH

The initial pH values is an important factor in metal ion sorption as it influences both the surface chemistry of MOCS adsorbent as well as the solution chemistry of U(VI) ions. The relative abundance of various U(VI) species is a strong function of pH and composition of solution. In the absence of carbonates, complexation of U(VI) and hydroxyl ion is a possible reaction, while in the presence of carbonates, the reaction of uranyl ion with CO_3^{2-} is the most dominant reaction in aqueous medium.

The no precipitate of U(VI) and colloid formation were observed in the pH range of 2.0–11.0 under the experimental condition. The experimental results are shown in Fig. 3. As shown in Fig. 3, the pH of aqueous phase is a controlling factor in U(VI) adsorption. Under higher acidic conditions, U(VI) uptake was minimal. As pH increased from 2.0 to 6.0, the fraction of U(VI) adsorbed on MOCS increased. Adsorption reached a maximum at pH of 6.0. The extent of adsorption diminished as pH continued to rise from 6.0 to 11.0. Therefore, all the adsorption experiments were carried out at pH 6.0.

Such a pH-dependence of U(VI) ions sorption on MOCS is similar to that for U(VI) adsorption on ferrihydrite, hematite, goethite, and amorphous iron hydroxide with solutions exposing to the atmosphere [17–20]. This behavior may be explained by that the carbonate concentration increases with pH at a constant carbon dioxide partial pressure, resulting in an increase in the concentration of soluble U(VI) carbonate complexes. The behavior of U(VI) ions in

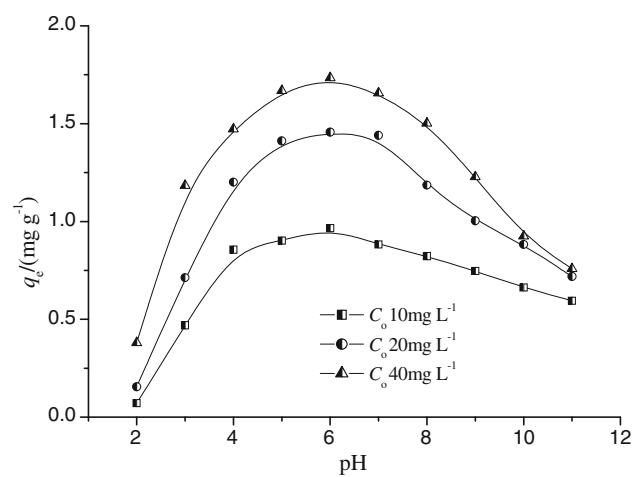


Fig. 3 Effect of initial pH on adsorption of U(VI) by MOCS

aqueous solution is a complex phenomenon in the sense that U(VI) ions may be present as ions of different composition. U(VI) basically exists as free uranyl ion, its hydrolysis complexes, and multinuclear hydroxide and carbonate complexes as a function of pH and U(VI) concentration under experimental conditions. At pH 7.0–10.0, the solution carbonate complexes of UO_2^{2+} such as $\text{UO}_2(\text{CO}_3)_2^{2-}$ and $\text{UO}_2(\text{CO}_3)_3^{4-}$, are the dominant anion species. They compete with U(VI) ions for adsorption sites, so that the adsorption of U(VI) ions decreases as the concentration of dissolved carbonate and bicarbonate anions increase [21].

Effect of salt concentration on U(VI) adsorption

The results obtained for the adsorption of U(VI) ions onto MOCS surface in the presence of NaNO_3 , $\text{Ca}(\text{NO}_3)_2$ are depicted in Fig. 4. It was seen that, irrespective of the nature of the salt, an increase in its concentration resulted in a decrease in the values of q_e for U(VI) ions studied. The trend indicates that the binding efficiency decreased when the salt concentration in metal ion solution increased, which may be attributed to competitive adsorption between the U(VI) ions

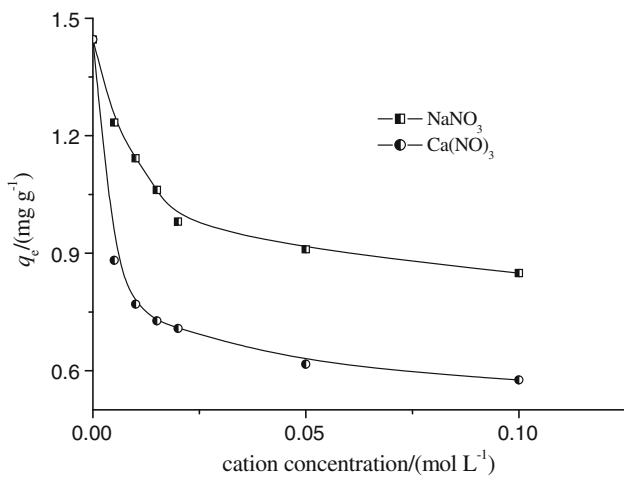


Fig. 4 Effect of salt concentrations on adsorption U(VI) ions

and the salt cations for the sites available on the adsorbent surface. Another factor was that increasing the salt concentration led to an increase in the ionic strength of the solution, so that the effective concentration (or activity) of the U(VI) ions in the solution decreased. Because of their greater positive charge, Ca^{2+} ions make a greater contribution to the ionic strength than Na^+ ions, leading to a greater influence by these ions on the adsorption process than Na^+ ions at the same molar concentration [10].

Effect of copper and zinc competition on U(VI) adsorption

The effect of different levels of Cu(II) and Zn(II) on the adsorption of U(VI) were demonstrated in Figs. 5 and 6, respectively. From Figs. 5 and 6, a significant decrease in U(VI) uptake was observed even at relatively low Cu(II) or Zn(II) concentrations. When the concentration of Cu(II)

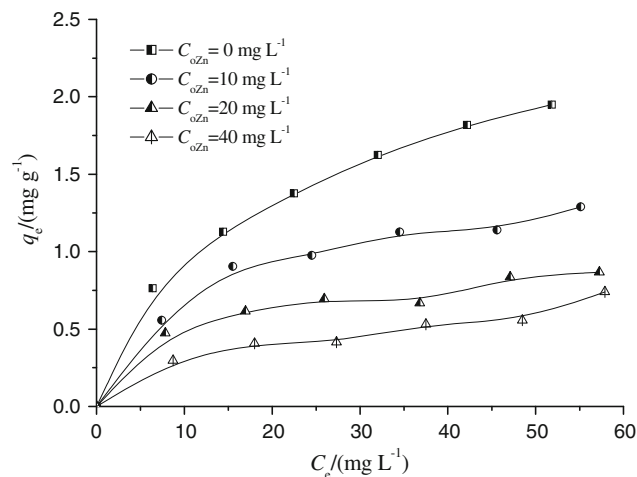


Fig. 6 Effect of various Zn(II) concentrations on adsorption U(VI)

increased from 0 to 40 mg L⁻¹, the adsorption quantity of q_e (UO_2^{2+}) decreased from 1.95 to 0.64 mg g⁻¹ and the maximum adsorption efficiency of U(VI) was reduced 67%. When the concentration of Zn(II) increased from 0 to 40 mg L⁻¹, the q_e (UO_2^{2+}) decreased from 1.95 to 0.74 mg g⁻¹ and the maximum adsorption efficiency reduced 62%. The results indicated that the competition occurred in the bi-solute sorption systems of Cu(II) and U(VI) or Zn(II) and U(VI) on MOCS.

Adsorption equilibrium study

The effect of the initial concentration of U(VI) ions in aqueous solutions on their equilibrium adsorption values at 288, 303 and 318 K is shown in Fig. 7.

As seen from this Fig. 7, the equilibrium uptakes of U(VI) ions increased as the initial concentrations of U(VI) ions in the system increased over the range of experimental

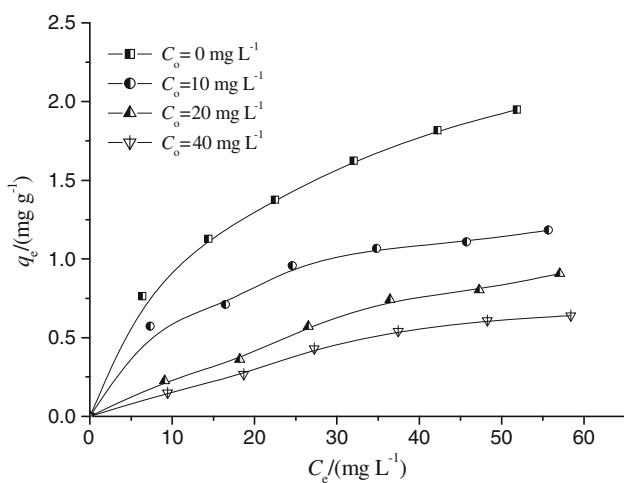


Fig. 5 Effect of various Cu(II) concentrations on adsorption U(VI)

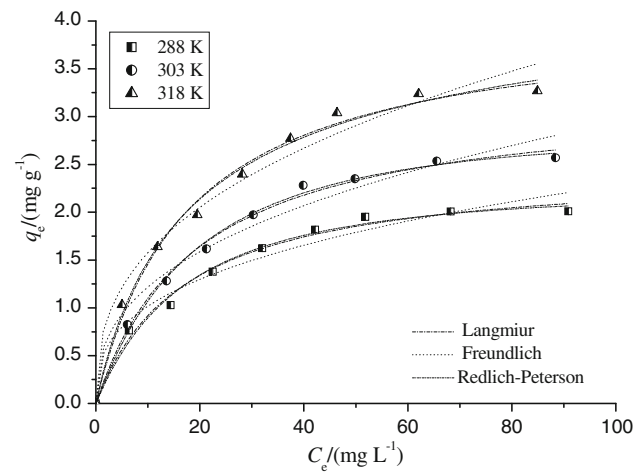


Fig. 7 Equilibrium adsorption quantities of U(VI) ions at different initial concentrations and predicted isotherm curves

concentration studied. In addition, the adsorption capacity of MOCS towards U(VI) ions increased with increasing temperature. This increase in the equilibrium uptake with increasing temperature indicates that the adsorption of U(VI) ions was endothermic in nature, suggesting the possibility that the adsorption process may be chemical in nature [11, 22].

To optimize the design of an adsorption system for the removal of adsorbate, it is important to establish the most appropriate correlation for the equilibrium data. In this paper, the Langmuir [23], Freundlich [24] and Redlich–Peterson [25] isotherm models were adopted.

The Langmuir adsorption isotherm has been successfully applied to many pollutants adsorption processes and has been the most widely used sorption isotherm for the sorption of a solute from a liquid solution. The common form of the Langmuir isotherm is:

$$q_e = \frac{q_m K_L C_e}{1 + K_L C_e} \quad (2)$$

where q_m is the q_e for a complete monolayer (mg g^{-1}), a constant related to adsorption capacity; and K_L is a constant related to the affinity of the binding sites and energy of adsorption (L mg^{-1}).

The Freundlich isotherm is an empirical equation describing adsorption onto a heterogeneous surface. The Freundlich isotherm is commonly presented as:

$$q_e = K_F C_e^{1/n} \quad (3)$$

where K_F and $1/n$ are the Freundlich constants related to the adsorption capacity and adsorption intensity of the adsorbent, respectively.

The three-parameter Redlich–Peterson equation which has a linear dependence on concentration in the numerator and an exponential function in the denominator has been proposed to improve the fit by the Langmuir or Freundlich equation and is given by Eq. 4:

$$q_e = \frac{K_{RP} C_e}{1 + a_{RP} C_e^g} \quad (4)$$

where K_{RP} , a_{RP} and g are the Redlich–Peterson parameters, g lies between 0 and 1. For $g = 1$, Eq. 4 converts to the Langmuir form.

The relative parameters of each equation are obtained using χ^2 between the calculated data and experimental data by nonlinear regressive analysis. The calculated expression of χ^2 is as follows:

$$\chi^2 = \sum \frac{(q_{e,\text{exp}} - q_{e,\text{cal}})^2}{q_{e,\text{cal}}} \quad (5)$$

where $q_{e,\text{cal}}$ is the predicted (calculated) quantity of U(VI) ions adsorbed onto MOCS according to adsorption models and $q_{e,\text{exp}}$ is the experimental data.

Table 1 Isotherm parameters for U(VI) ions adsorption on MOCS

Model	283 K	293 K	303 K
<i>Langmuir</i>			
K_L	0.0498 ± 0.007	0.0516 ± 0.100	0.0563 ± 0.006
q_m (mg/g)	2.483 ± 0.097	3.234 ± 0.005	4.050 ± 0.151
R^2	0.9902	0.9949	0.9923
χ^2	0.084	0.018	0.043
<i>Freundlich</i>			
K_F	0.453 ± 0.074	0.504 ± 0.082	0.657 ± 0.090
$1/n$	0.351 ± 0.042	0.383 ± 0.042	0.380 ± 0.036
R^2	0.9701	0.9731	0.9793
χ^2	0.072	0.092	0.084
<i>Redlich–Peterson</i>			
K_{RP}	0.128 ± 0.025	0.145 ± 0.019	0.258 ± 0.062
a_{RP}	0.036 ± 0.028	0.029 ± 0.017	0.086 ± 0.062
g	0.967 ± 0.134	1.095 ± 0.102	0.936 ± 0.108
R^2	0.9907	0.9955	0.9927
χ^2	0.036	0.022	0.034

All relative parameters of isotherm equation and determined coefficients (R^2), values of χ^2 are listed in Table 1, respectively. Figure 7 also shows the experimental equilibrium data and fitted equilibrium curve by three various isotherms at different temperature, respectively.

From Table 1, the adsorption capacity of MOCS (q_m) increased on increasing the temperature. The values of q_m obtained at 283, 293, 303 are 2.48 , 3.23 , 4.05 mg g^{-1} , respectively.

Examination of the data showed that the Redlich–Peterson isotherm is an appropriate description of the data for U(VI) ions adsorption over the concentration ranges studied. The constant g is near to 1, and these indicate the isotherm is approaching the Langmuir form.

From Table 1, all measure values of K_F showed easy uptake of U(VI) with high adsorptive capacity of MOCS and significant differences in adsorption capacities due to temperature. The obtained values of $1/n$ ($0.1 < 1/n < 1$) indicated a higher adsorb ability of U(VI) at all temperatures studied [22]. The results also indicated that with the temperature increasing, the ability of adsorption increased. Based on the values of R^2 , χ^2 , and from Fig. 7, the non-linear forms of the Langmuir, Freundlich and Redlich–Peterson isotherms appear to produce a better model for adsorption in U(VI)/MOCS systems.

Adsorption kinetic study

The rate of U(VI) adsorption on MOCS was determined as a function of the initial U(VI) ions concentrations. The uptake of U(VI) ions for three initial U(VI) concentrations at different contact time is listed in Fig. 8. The results

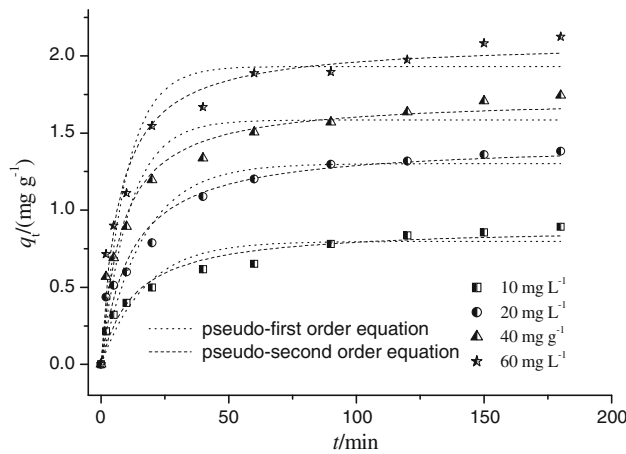


Fig. 8 Effect of initial U(VI) concentration on adsorption kinetics and fitted curves

showed that kinetics of adsorption of U(VI) ions consisted of two phases: an initial rapid phase where adsorption was fast and contributed significant to equilibrium uptake and a slower second phase whose contribution to the total U(VI) ions adsorption was relatively small [26, 27]. The first phase is the instantaneous adsorption stage or external surface adsorption. The second phase is the gradual adsorption stage and finally U(VI) ions uptake reached equilibrium. As seen from Fig. 8, a higher initial concentration of U(VI) increase the adsorption capacity. It was also seen that equilibrium time occurred relatively earlier

in the solution containing lower U(VI) concentrations than the higher ones. The necessary time to reach equilibrium is variable according to the initial concentration.

In order to investigate the adsorption kinetics of U(VI) on MOCS, the pseudo-first order kinetic model, pseudo-second order kinetic model and intraparticle diffusion model were applied.

The pseudo-first-order kinetic model is expressed as [28]:

$$q_t = q_e (1 - e^{-k_1 t}) \quad (7)$$

The pseudo-second-order kinetic model is given by the following equation as [28, 29]:

$$q_t = \frac{k_2 q_e^2 t}{1 + k_2 q_e t} \quad (8)$$

where q_e and q_t are the amount of U(VI) adsorbed per unit weight of the adsorbent at equilibrium and at any time t , respectively (mg g^{-1}) and k_1 is the rate constant of pseudo-first order adsorption (min^{-1}); k_2 is the rate constant of pseudo-second order adsorption ($\text{g mg}^{-1} \text{ min}^{-1}$).

Table 2 presents the results of fitting experimental data with pseudo-first order and pseudo-second order equations using nonlinear analysis. The fitted curves are also shown in Fig. 8. Table 2 Kinetic parameters of U(VI) ions adsorption onto MOCS.

From Table 1, the value of R^2 (0.963) from the pseudo-second order kinetic model was higher than that from the

Table 2 Kinetic parameters of U(VI) ions adsorption onto MOCS

C_o (mg L^{-1})	10	20	40	60
<i>Pseudo-first order equation</i>				
k_1 (min^{-1})	0.058 ± 0.013	0.061 ± 0.012	0.091 ± 0.017	0.102 ± 0.019
$q_{e(\text{cal})}$ (mg g^{-1})	0.797 ± 0.042	1.302 ± 0.012	1.584 ± 0.065	1.932 ± 0.075
$q_{e(\text{exp})}$ (mg g^{-1})	0.891	1.382	1.744	2.124
R^2	0.9128	0.9300	0.9318	0.9360
χ^2	0.321	0.674	0.448	0.446
<i>Pseudo-second order equation</i>				
k_2 ($\text{g mg}^{-1} \text{ min}^{-1}$)	0.088 ± 0.021	0.076 ± 0.014	0.074 ± 0.014	0.070 ± 0.012
$q_{e(\text{cal})}$ (mg g^{-1})	0.892 ± 0.040	1.409 ± 0.061	1.730 ± 0.054	2.094 ± 0.061
R^2	0.9627	0.9636	0.9748	0.9760
χ^2	0.118	0.203	0.157	0.155
<i>Intra-particle diffusion model</i>				
K_{t1} ($\text{mg g}^{-1} \text{ min}^{-0.5}$)	0.066 ± 0.005	0.113 ± 0.008	0.150 ± 0.014	0.186 ± 0.020
C_1 (mg g^{-1})	0.169 ± 0.026	0.270 ± 0.043	0.398 ± 0.067	0.520 ± 0.098
R	0.9879	0.9894	0.9829	0.9766
χ^2	0.090	0.185	0.447	0.684
K_{t2} ($\text{mg g}^{-1} \text{ min}^{-0.5}$)	0.027 ± 0.003	0.030 ± 0.004	0.044 ± 0.002	0.046 ± 0.008
C_2 (mg g^{-1})	0.533 ± 0.037	0.985 ± 0.045	1.164 ± 0.020	1.497 ± 0.086
R^2	0.9863	0.9736	0.9973	0.9588
χ^2	0.484	0.936	0.769	0.963

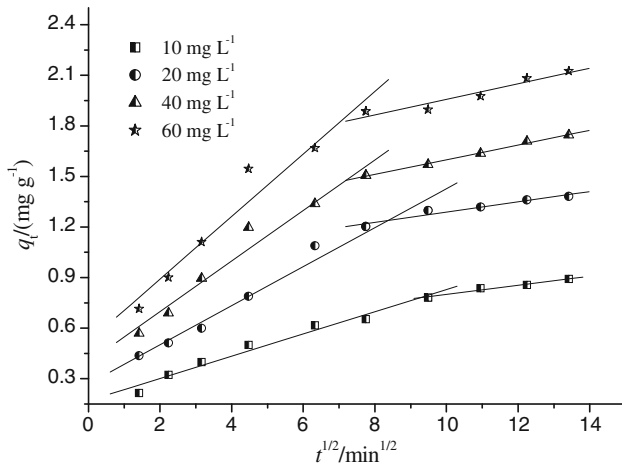


Fig. 9 Intra-particle diffusion plots for U(VI) ions adsorption of onto MOCS

pseudo-first order kinetic model while χ^2 was smaller. The fitted curve from the pseudo-second order kinetic model was very close to the experimental curve (see Fig. 8). So it was concluded that the pseudo-second order kinetic model is better to fit the experimental data and the process may be chemical process [28].

Mechanism of adsorption

The adsorbate transport from the solution phase to the surface of the adsorbent particles occurs in several steps. The overall adsorption process may be controlled either by one or more steps, e.g., film or external diffusion, pore diffusion, surface diffusion and adsorption on the pore surface, or a combination of more than one step. The possibility of intra-particle diffusion was explored by using the intra-particle diffusion model [30]:

$$q_t = Kt^{1/2} + C \quad (9)$$

K is the intraparticle diffusion rate constant ($\text{g mg}^{-1} \text{min}^{-1/2}$), C is a constant that gives idea about the thickness of the boundary layer.

Figure 9 presented the plots of q_t versus $t^{1/2}$ for U(VI) ions adsorption on MOCS. It is clear that the plots are two-linear, containing at least two linear segments. The regression results are presented in Table 2. For all the two-linear plots in Fig. 9, the regression estimates of the first linear segments had intercept values different from zero suggesting that pore diffusion be not the step controlling the overall rate of mass transfer at the beginning of batch adsorption. Film-diffusion control may have taken place and ended in the early stages of adsorption, or maybe it is still controlling the rate of mass transfer in the time period of the first linear segment [31]. This shows that the

mechanism of U(VI) ions adsorption on MOCS is complex and both the surface adsorption and intraparticle diffusion contribute to the actual adsorption process.

The half-adsorption time $t_{1/2}$ was another parameter which can be calculated from the equilibrium concentration and the diffusion coefficient rate values. This was calculated by using the following equation [32]:

$$t_{1/2} = \frac{1}{k_2 q_e} \quad (10)$$

where k_2 and q_e can be obtained from Table 2. The diffusion coefficient for the intraparticle transport of U(VI) ions was also calculated by using the following relationship [32]:

$$t_{1/2} = \frac{0.03r^2}{D} \quad (11)$$

where $t_{1/2}$ is the half life in seconds as calculated from Eq. 10, r is the radius of the adsorbent particle in centimeters and D is the diffusion coefficient value in $\text{cm}^2 \text{s}^{-1}$. For the calculation of the r value, it is assumed that the solid phase consists of particles which are spherical in nature. The calculated values of $t_{1/2}$ were 12.7, 9.3, 7.8 and 7.8 min^{-1} , while the calculated values of D were 1.47×10^{-7} , 2.01×10^{-7} , 2.41×10^{-7} and $2.75 \times 10^{-7} \text{ cm}^2 \text{s}^{-1}$ at initial U(VI) concentration of 10, 20, 40 and 60 mg L^{-1} , respectively. The values of pore diffusion rate constants are found to be on the order of 10^{-10} – $10^{-11} \text{ cm}^2 \text{s}^{-1}$ for all the adsorbent samples, so the pore diffusion in this study was not significant [32].

Estimation of thermodynamic parameters

In adsorption studies, both energy and entropy factors must be considered in order to determine which process will occur spontaneously. The Gibbs free energy change, ΔG , can be determined by the following equation [22, 33]:

$$\Delta G = -RT \ln K'_c \quad (12)$$

$$\Delta G = \Delta H - T\Delta S \quad (13)$$

The apparent equilibrium constant (K'_c) of the adsorption is defined as:

$$K'_c = \frac{C_{\text{ad,e}}}{C_e} \quad (14)$$

where $C_{\text{ad,e}}$ is the concentration of U(VI) ions on the adsorbent at equilibrium (mg L^{-1}). The value of K'_c in the lowest experimental U(VI) concentration can be obtained [33]. The K'_c value is used in the Eq. 12 to determine the change of Gibbs free energy of adsorption. The values of ΔG were presented in Table 3. Enthalpy change, ΔH , and entropy change, ΔS , were determined from the slope and intercept of the plot according to Eq. 12.

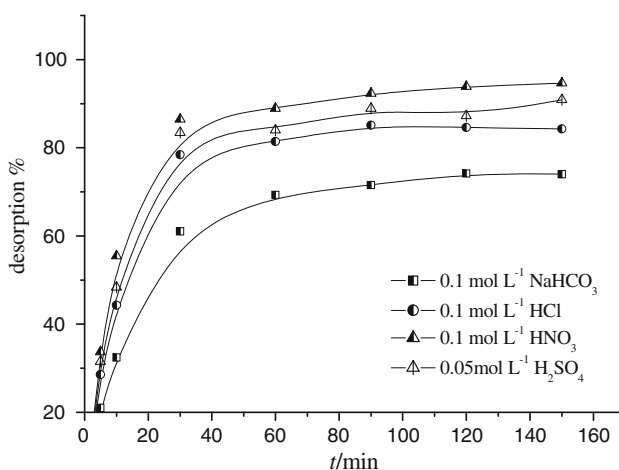
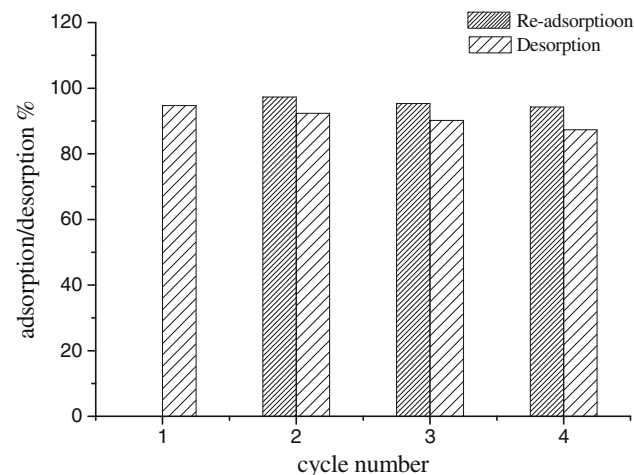
Table 3 Thermodynamic parameters adsorption of U(VI) ions by MOCS

<i>T</i> (K)	288 K	303 K	318 K
ΔG (kJ mol ⁻¹)	-9.36	-9.93	-10.66
ΔH (kJ mol ⁻¹)		3.318	
ΔS (J mol ⁻¹ K ⁻¹)		44.3	

The negative value of ΔG is due to the fact that the adsorption process is spontaneous and the negative value of ΔG decreased with an increase in temperature. The positive values of ΔH suggest the endothermic nature of the adsorption of U(VI) on MOCS whereas the positive ΔS values indicate the increased randomness at the solid-liquid interface during the adsorption of U(VI) onto MOCS. The low values of ΔS also indicated that no remarkable change on entropy occurs.

Desorption studies

In order to estimate the metal releasing capacity of MOCS loaded with U(VI), desorption experiments were carried out in a batch system. The regeneration of the adsorbent can be achieved by washing loaded adsorbent with an appropriate desorbing solution that must be cheap, effective, non-polluting and non-damaging to the adsorbent, so various solution of HNO_3 , H_2SO_4 , HCl and $NaHCO_3$ were tested as desorbing agent for previously adsorbed U(VI) ions on MOCS (Fig. 10). It was found that U(VI) ions desorption was 94.7, 90.9, 84.3 and 74.0% with HNO_3 , H_2SO_4 , HCl and $NaHCO_3$, respectively. Therefore 0.1 mol L⁻¹ HNO_3 solution was selected as an eluent to desorb the U(VI) ions from metal-loaded MOCS in this study.

**Fig. 10** Plots of the desorption of U(VI) ions from spent MOCS under different desorbing agent**Fig. 11** Four cycles of U(VI) ions adsorption–desorption with 0.1 mol L⁻¹ HNO_3 as the desorbing agent

In order to show the reusability of the sorbent, adsorption–desorption cycle of U(VI) ions was repeated four times using the same preparations and the results were shown in Fig. 11. There was a decrease in both the amount of U(VI) ions adsorbed and the amount of U(VI) ions desorbed from the first to the fourth cycle. At the end of the fourth cycle, there was a decrease of 13% efficiency for both the adsorption and desorption processes. This showed that MOCS was restored close to the original condition without damage to the nature of the adsorption characteristics of the adsorbent.

Comparison with virgin sand and other solid adsorbents

The respective adsorption capacities of quartz sand and MOCS towards U(VI) ions are listed in Table 4 as 0 and

Table 4 Comparison of adsorption/retention capacities of MOCS and various adsorbents for U(VI) ions

Adsorbent	pH	Adsorption capacity (mg g ⁻¹)	Reference
Virgin sand	5.0	0	This study
MOCS	5.0	3.23	This study
Silica gel	5.15	97.9	[35]
Diatomite	5.0	38.6	[36]
Hematite	2.78	3.36	[37]
Magnetite	7.00	5.0	[38]
Natural zeolite material	2.78	8.70	[12]
Goethite-coated sand	9	0.624	[39]
Alumina	6.5	9.95	[40]
Polyacryloamidoxime resin-coated quartz sand	6.0	1.0	[41]
Activated carbon prepared from charcoal.	5	28.5	[42]
Modified clays with titanium oxide	3.50	0.582	[43]

3.23 mg g⁻¹ at 293 K. This enhancement in adsorption capacity is attributed to the high negative surface charge on the modified surface [11, 34]. Furthermore, the increase in the surface area is assumed to play a significant role in the overall removal process [11].

Various forms of natural and synthetic adsorbents have been used for the removal of heavy metal ions from aqueous solutions and wastewaters, with the adsorption of U(VI) ions onto various minerals being widely described in the literature. Table 4 also provides a comparison of the U(VI) ion uptake capacities of some natural and synthetic adsorbents, based on mg U(VI) ion adsorbed per g of adsorbent. It will be seen from Table 4 that the adsorption capacity of MOCS was lower than that of natural and modified minerals reported in the literature to date except that of goethite-coated sand, polyacryloamidoxime resin-coated quartz sand and modified clays with titanium oxide. However, more than 95% U(VI) ions may be easily eluted from the MOCS column, with the efficiency towards U(VI) adsorption remaining virtually unchanged in the following cycles. Hence, MOCS may be considered as an excellent adsorbent for U(VI) ions with promising potential applications for the removal of these ions from industrial effluents.

Conclusions

In this study, the adsorption of U(VI) ions on MOCS from aqueous solutions was investigated by batch technique. The results showed MOCS is an effective adsorbent for U(VI) ions removal from aqueous solutions. The binding U(VI) ions capacity by MOCS was strongly dependent on the initial pH, initial U(VI) ions concentration and temperature. It was noted that an increase in the temperature resulted in a higher metal loading per unit weight of MOCS. The sorption isotherms of U(VI) ions sorbed on MOCS followed the Langmuir and Redlich–Peterson models. Kinetics data tend to fit well in pseudo-second-order kinetic models. The process was spontaneous and endothermic. Desorption studies conducted showed that U(VI) ions adsorbed onto MOCS could be desorbed effectively using 0.1 mol L⁻¹ HNO₃ and the spent MOCS could be reused several times after regeneration. It indicated that MOCS can be used as an effective adsorbent for the treatment of industrial wastewaters contaminated with U(VI) ions.

Acknowledgments The authors express their sincere gratitude to Henan Science and Technology Department and to the Education Department of Henan Province in P.R. China for the financial support of this study (Nos. 102102210103 and 2010A610003).

References

1. Domia AM, Atia AA, Moussa MM, Sherif AM, Magied MO (2009) Hydrometallurgy 95:183
2. Ganesh R, Robinson KG, Chu LL, Kucsmas D, Reed GD (1999) Water Res 33:3447
3. Kryvoruchko AP, Yurlova LY, Atamanenko ID, Kornilovich BY (2004) Desalination 162:229
4. Mellah A, Chegrouche S, Barkat M (2006) J Colloid Interface Sci 296:434
5. Sodaya H, Nisanb S, Poletikoc C, Prabhakara S, Tewaria PK (2009) Desalination 235:9
6. Jenne EA (1968) In: Gould RF (ed) Trace inorganics in water. American Chemical Society, Washington, DC, p 337
7. Coughlin B, Stone A (1995) Environ Sci Technol 29:2445
8. Al-Degs Y, Khrasheh MAM, Tutunji MF (2001) Water Res 35:3724
9. Boujelben N, Bouzid J, Elouear Z (2009) Adsorpt Sci Technol 27:177
10. Han RP, Zou WH, Zhang ZP, Shi J, Yang JJ (2006) J Hazard Mater 137:384
11. Zou WH, Han RP, Chen ZZ, Shi J, Liu HM (2006) J Chem Eng Data 51:534
12. Misaelides P, Godelitsas A, Filippidis A, Charistos D, Anousi I (1995) Sci Total Environ 173/174:237
13. Liu DF, Teng Z, Sansalone JJ, Cartledge Fkj (2001) Environ Eng ASCE 127:879
14. Kim JG, Dixon JB, Chusuei CC, Deng Y (2002) Soil Sci Soc Am J 66:306
15. Metilda P, Sanghamitra K, Mary Gladis J, Naidu GRK, Prasada Rao T (2005) Talanta 65:192
16. Bontea D, Mita C, Humelnicu D (2006) J Radioanal Nucl Chem 268:305
17. Anirudhan TS, Divya L, Suchithra PS (2009) J Environ Manag 90:549
18. Lenhart JJ, Honeyman BD (1999) Geochim Cosmochim Acta 63:2891
19. Waite TD, Davis JA, Payne TE, Waychunas GA, Xu N (1994) Geochim Cosmochim Acta 58:5465
20. Wazne M, Korfiatis GP, Meng X (2003) Environ Sci Technol 37:3619
21. Barnett MO, Jardine PM, Brooks SC, Selim HM (2000) Soil Sci Soc Am J 64:908
22. Aksu Z (2002) Process Biochem 38:89
23. Langmuir I (1916) J Am Chem Soc 38:2221
24. Freundlich HMF (1906) Z Phys Chem 57:385
25. Fu XC, Shen WX, Yao TY (1994) Physical chemistry, 4th edn. Higher Education Press, China, p 303
26. Han RP, Zhang JJ, Han P, Wang YF, Zhao ZH, Tang MS (2009) Chem Eng J 145:496
27. Wang SB, Ariyanto E (2007) J Colloid Interface Sci 314:25
28. Ho YS, Ng JCY, McKay G (2000) Sep Purif Methods 29:189
29. Ho YS, McKay G (1999) Process Biochem 34:451
30. Cheung CW, Porter JF, McKay G (2000) Sep Purif Technol 19:55
31. Srivastava VC, Swamy MM, Mall ID, Prasad B, Mishra IM (2006) Colloid Surf A 272:89
32. Dogan M, Ozdemir Y, Alkan M (2007) Dyes Pigments 75: 701–713
33. Catts JG, Langmuir D (1986) Appl Geochem 1:255
34. Kanungo SB, Paroda KM (1984) J Colloid Interface Sci 98:252
35. Tran HH, Roddick FA, O'Donnell JA (1999) Water Res 33:2992
36. Xie SB, Zhang C, Zhou XH, Yang J, Zhang XJ, Wang JS (2009) J Environ Radioact 100:162

37. Ölmez S, Aytaş S, Akyil MAA, Aslani U (1999) Nucl Chem 240:973
38. Das D, Sureshkumar MK, Koley S, Mithal N, Pillai CGS (2010) J Radioanal Nucl Chem 285:447
39. Gabriel U, Gaudet JP, Spadini L, Charlet L (1998) Chem Geol 151:107
40. Sylwester ER, Hudson EA, Allen PG (2000) Geochim Cosmochim Acta 64:2431
41. Barton CS, Stewart DI, Morrisb K, Bryant DE (2004) J Hazard Mater 116:191
42. Kütahyal C, Eral M (2004) Sep Purif Technol 40:109
43. Humelnicu D, Popovici E, Dvininov E, Mita C (2009) J Radioanal Nucl Chem 279:131